*Catalysis Letters Vol. 99, Nos. 3–4, February 2005 (© 2005)*
DOI: 10.1007/s10562-005-2130-8


# Correlation between acidic properties of nickel sulfate supported on $TiO_2$-$ZrO_2$ and catalytic activity for ethylene dimerization

Young Il Pae,[1,2,*] Si Hoon Lee[1] and Jong Rack Sohn[1]

[1]*Department of Applied Chemistry, Engineering College Kyungpook National University, Taegu 702-701, Korea*
[2]*Department of Chemistry, University of Ulsan, Ulsan 680-749, Korea*

Received 12 August 2004; accepted 12 October 2004

A series of catalysts, $NiSO_4/TiO_2$-$ZrO_2$, for ethylene dimerization was prepared by the impregnation method using an aqueous solution of nickel sulfate. For $NiSO_4/TiO_2$-$ZrO_2$ sample, no diffraction line of nickel sulfate was observed up to 30 wt%, indicating good dispersion of nickel sulfate on the surface of $TiO_2$-$ZrO_2$. The addition of nickel sulfate to $TiO_2$-$ZrO_2$ shifted the phase transition of $TiZrO_4$ from amorphous to orthorhombic to a higher temperature because of the interaction between nickel sulfate and $TiO_2$-$ZrO_2$. The number of acid sites of $NiSO_4/TiO_2$-$ZrO_2$ increased in proportion to the nickel sulfate content up to 20 wt% of $NiSO_4$. Nickel sulfate supported on $TiO_2$-$ZrO_2$ was found to be very active even at room temperature, giving a maximum in both activity and acidity, when the catalyst containing 20% $NiSO_4$ was calcined and evacuated at 500 °C. The asymmetric stretching frequency of the S=O bonds for $NiSO_4/TiO_2$-$ZrO_2$ samples was related to the acidic properties and catalytic activity. That is, the higher the frequency, the higher both the number of acid sites and the catalytic activity for ethylene dimerization.

**KEY WORDS:** ethylene dimerization; $NiSO_4/TiO_2$-$ZrO_2$; acid strength; acidity; $TiZrO_4$ compound; asymmetric S=O stretching frequency.

## 1. Introduction

Heterogeneous catalysts for the dimerization and oligomerization of olefins, consisting mainly of nickel compounds supported on oxides, have been known for many years. A considerable number of papers have dealt with the problem of nickel-containing catalysts for ethylene dimerization [1–12]. One of the remarkable features of this catalyst system is its activity in relation to a series of *n*-olefins. In contrast to usual acidic catalysts, nickel oxide on silica or silica-alumina shows a higher activity for lower olefin dimerization, particularly for ethylene [1–6,11]. It has been reported that the dimerization activities of such catalysts are related to the acidic property of surface and low valent nickel ions. In fact, nickel oxide, which is active for $C_2H_4$–$C_2D_4$ equilibration, acquires an activity for ethylene dimerization upon addition of nickel sulfate, which is known to be an acid [13]. A transition metal can also be supported on zeolite in the state of a cation or a finely dispersed metal. Several papers have treated ethylene dimerization on transition-metal cation exchanged zeolites [14–16].

However, binary metal oxides are expected to exhibit better catalytic activity for some reaction due to their solid acid or base properties [17]. Among various binary oxide, the $TiO_2$-$ZrO_2$ exhibited very good catalytic activity. The $TiO_2$-$ZrO_2$ binary oxide has also been reported to exhibit high surface acidity by a charge imbalance based on the generation of Ti–O–Zr bonding [18]. Further, recent studies also reveal that $TiO_2$-$ZrO_2$ is an active catalyst for dehydrocyclization of *n*-paraffins to aromatics [19], hydrogenation of carboxylic acids to alcohols [20] and photo catalytic oxidation of acetone [21], and also is an effective support for $MoO_3$-based catalysts for hydroprocessing application [22]. Thus, the mixed $TiO_2$-$ZrO_2$ oxide has attracted attention recently as a catalyst and support for various applications.

In this investigation, a $TiO_2$-$ZrO_2$ binary oxide support was prepared by a co-precipitation method and was used as a support. As an extension of our study on ethylene dimerization, we also prepared other catalyst systems by supporting nickel sulfate on $TiO_2$-$ZrO_2$ binary oxide. In this paper, a correlation between the acidic properties of nickel sulfate supported on $TiO_2$-$ZrO_2$ and the catalytic activity for ethylene dimerization are reported.

## 2. Experimental

### 2.1. Catalysts

The $TiO_2$-$ZrO_2$ mixed oxide (1:1 mole ratio) was prepared by a co-precipitation method using ammonium hydroxide (2.7 N) as the precipitation reagent. The co-precipitate of $Ti(OH)_4$-$Zr(OH)_4$ was obtained by adding ammonium hydroxide slowly into a mixed aqueous solution of titanium tetrachloride and zirconium oxychloride (Junsei Chemical Co.) at 60 °C with stirring until the pH of mother liquor reached about 8. The

co-precipitate thus obtained was washed thoroughly with distilled water until chloride ion was not detected, and was dried at 100 °C for 12 h. Catalysts containing various nickel sulfate contents were prepared by dry impregnation of $Ti(OH)_4$-$Zr(OH)_4$ powder with an aqueous solution of $NiSO_4 \cdot 6H_2O$ followed by calcining at different temperatures for 1.5 h in air. It was used as a catalyst after evacuation at different temperatures for 1 h. This series of catalysts is denoted by the weight percentage of nickel sulfate. For example, 20-$NiSO_4$/$TiO_2$-$ZrO_2$ indicates the catalyst containing 20 wt% of $NiSO_4$.

### 2.2. Procedure

The catalytic activity for ethylene dimerization was determined at 20 °C using a conventional static system by following the pressure change with an initial pressure set at 290 Torr. A fresh catalyst sample of 0.2 g was used for every run, and the catalytic activity was calculated as the initial rate calculated from the initial activity slope. Reaction products were analyzed by gas chromatograph with a VZ-7 column at room temperature.

Chemisorption of ammonia was employed as a measure of the number of acid sites of each catalyst. The amount of chemisorption was obtained as the irreversible adsorption of ammonia [4,6,9]. The specific surface area was determined by applying the BET method to the adsorption of nitrogen at −196 °C.

X-ray diffractograms of catalysts were taken by a Philips X.pert-APD X-ray diffractometer (XRD) using a copper target and a nickel filter at 30 kV and 800 cps.

FT-IR (Fourier transform infrared) spectra were obtained in a heatable gas cell at room temperature using a Mattson Model GL6030E spectrometer. Self-supporting catalyst wafers contained about 9 mg/cm$^2$. Prior to obtaining the spectra, the samples were heated under vacuum at 100–700 °C for 1 h.

DSC measurements were performed in air using a PL-STA model 1500H apparatus, and the heating rate was 5 °C/min. For each experiment 10–15 mg of sample was used.

## 3. Results and discussion

### 3.1. Infrared spectra of $NiSO_4/TiO_2$-$ZrO_2$

In general, for the metal oxides modified with the sulfate ion followed by evacuating above 400 °C, a strong band assigned to S=O stretching frequency is commonly found in the range of 1360–1410 cm$^{-1}$ [9,23,24]. Infrared spectra of 20-$NiSO_4/TiO_2ZrO_2$ after evacuation at 25–600 °C for 1 h are shown in figure 1. There are sharp bands at 1350–1380 cm$^{-1}$ accompanied by four broad but split bands at 1213–1215, 1110–1121, 1059–1073 and 995–1010 cm$^{-1}$, indicating the presence

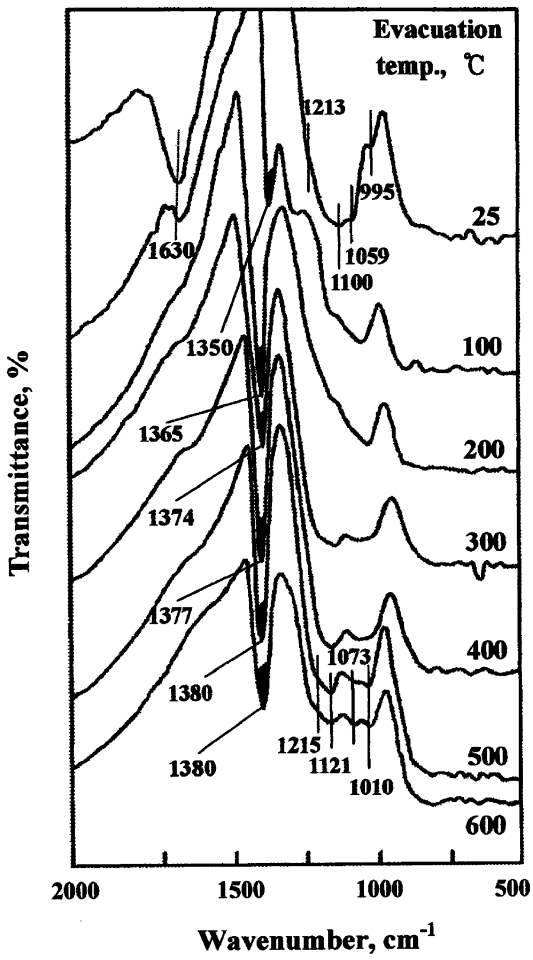


Figure 1. Infrared spectra of 20-$NiSO_4/TiO_2$-$ZrO_2$ evacuated at different temperatures.

of two kinds of sulfated species. The bands at 1350–1380 cm$^{-1}$ corresponds to the asymmetric S=O stretching frequency of sulfate ion bonded to $TiO_2$-$ZrO_2$ under the dehydrated condition, while the latter four bands are assigned to bidentate sulfate ion coordinated to $TiO_2$-$ZrO_2$ [9,22,23]. These results are very similar to those of other workers [23,25]. However, the frequency shift of this band is different depending on the evacuation temperature, as shown in figure 1. At 25 °C an asymmetric stretching band of S=O bonds was not observed because the water molecules are adsorbed on the surface of 20-$NiSO_4/TiO_2$-$ZrO_2$ [9,22,23]. The bands at 1630 cm$^{-1}$ are due to the $H_2O$ absorbed on the surface. However, at 100 °C the band began to appear at 1350 cm$^{-1}$ as a shoulder, and the band intensity increased with the evacuation temperature and the position of band shifted to a higher wavenumber up to 500 °C. That is, the higher the evacuation temperature, the larger the shift of the asymmetric stretching frequency of the S=O bonds. However, at 600 °C the band intensity decreased without further band shift because of desorption of sulfate ions. It is likely that the surface sulfur complexes formed by the interaction of oxides

with the sulfate ions in these highly active catalysts have a strong tendency to reduce their bond order by the adsorption of basic molecules, such as $H_2O$ [9,23,24]. Consequently, as shown in figure 1, an asymmetric stretching band of S=O bonds for the sample evacuated at lower temperature appears at a lower frequency compared with that for the sample evacuated at higher temperature. This is probably due to the fact that the adsorbed water reduces the bond order of S=O from a highly covalent double-bond character to a lesser double-bond character. The strong ability of the sulfur complex to accommodate electron from a basic molecule such as $H_2O$ is a driving force in generating superacidic properties [9,22,23].

### 3.2. Crystalline structure of $NiSO_4/TiO_2$-$ZrO_2$

The XRD patterns of the $TiO_2$-$ZrO_2$ support calcined at 500–1000 °C are shown in figure 2. As can be noted from this figure, the $TiO_2$-$ZrO_2$ mixed support is in an amorphous state up to its 600 °C calcination temperature. However, the formation of the crystalline $ZrTiO_4$ compound was observed at 700 °C, and the line intensity of this compound increased with the calcination temperature. Recently, Fung and Wang [19] also reported the formation of the $ZrTiO_4$ compound at 650 °C and above, coinciding with our XRD observations. As shown in figure 2, the $ZrTiO_4$ compound appears to be thermally quite stable even up to a 1000 °C calcination temperature.

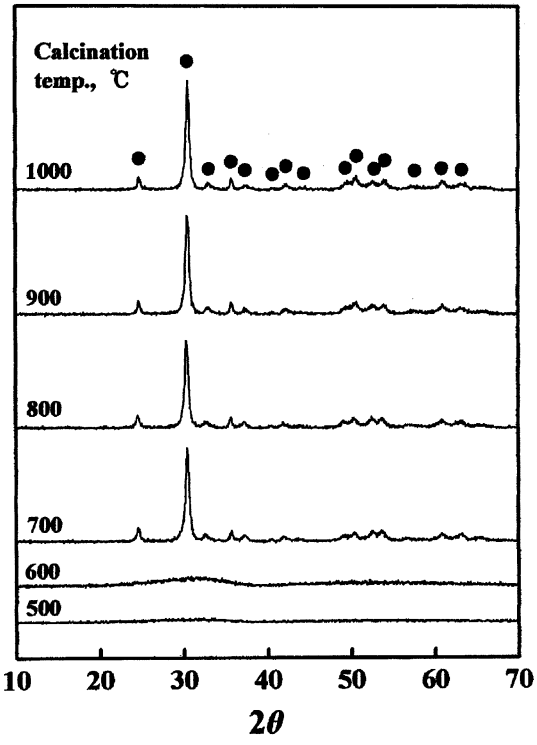


Figure 2. XRD patterns of $TiO_2$-$ZrO_2$ calcined at different temperatures: ●, orthorhombic phase of $TiZrO_4$.

The crystalline structure of 20- $NiSO_4/TiO_2$-$ZrO_2$ calcined in air at different temperatures for 1.5 h was checked by XRD (not shown in the figure). For the 20-z$NiSO_4/TiO_2$-$ZrO_2$, XRD data indicated only orthorhombic phase of $ZrTiO_4$ compound at temperatures of 700 °C and above without detection of orthorhombic $NiSO_4$ phase. However, in a separate experiment, for pure $NiSO_4$ calcined at 800 °C a cubic phase of nickel oxide was observed due to the decomposition of nickel sulfate, showing good agreement with the results of DSC described below. These results indicate that $NiSO_4$ supported on $TiO_2$-$ZrO_2$ is thermally more stable than unsupported $NiSO_4$. The other $NiSO_4/TiO_2$-$ZrO_2$ samples containing different $NiSO_4$ contents also exhibited results similar to that of 20-$NiSO_4/TiO_2$-$ZrO_2$.

### 3.3. Thermal analysis

To examine the thermal properties of precursors of $NiSO_4/TiO_2$-$ZrO_2$ samples more closely, thermal analysis has been carried out and the results are illustrated in figure 3. For pure $NiSO_4 \cdot 6H_2O$, the DSC curve shows three endothermic peaks below 400 °C due to water elimination, indicating that the dehydration of $NiSO_4 \cdot 6H_2O$ occurs in three steps. The endothermic

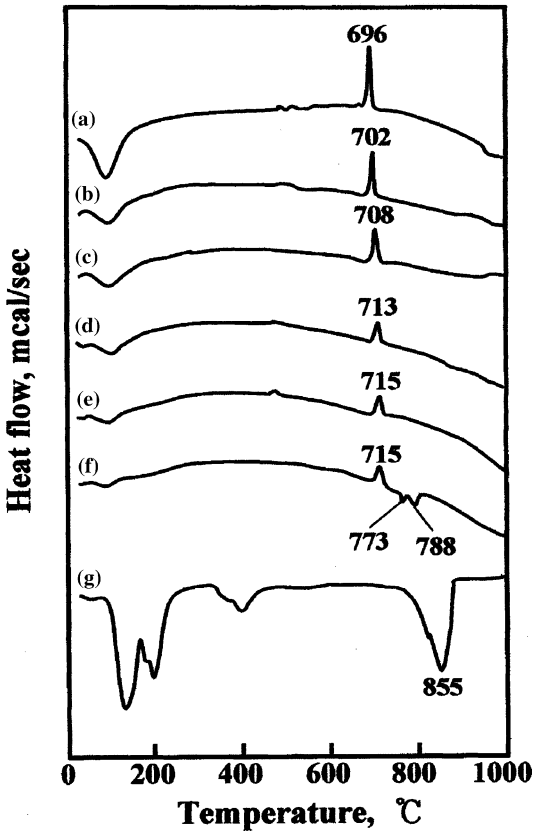


Figure 3. DSC curves of $NiSO_4/TiO_2$-$ZrO_2$ precursors having different $NiSO_4$ contents: (a) $TiO_2$-$ZrO_2$, (b) 5-$NiSO_4/TiO_2$-$ZrO_2$, (c) 10-$NiSO_4/TiO_2$-$ZrO_2$, (d) 15-$NiSO_4/TiO_2$-$ZrO_2$, (e) 20-$NiSO_4/TiO_2$-$ZrO_2$, (f) 30-$NiSO_4/TiO_2$-$ZrO_2$, and (g) $NiSO_4 \cdot 6H_2O$.

peak around 837 °C is due to the evolution of $SO_3$ decomposed from nickel sulfate [26]. Decomposition of nickel sulfate is known to begin at 700 °C [27].

However, for $TiO_2$-$ZrO_2$ and $NiSO_4/TiO_2$-$ZrO_2$ samples, the DSC patterns are somewhat different from that of $NiSO_4 \cdot 6H_2O$. For $TiO_2$-$ZrO_2$, the DSC curve shows a broad endothermic peak below 200 °C due to the elimination of adsorbed water, and a sharp and exothermic peak at 696 °C due to the formation of $ZrTiO_4$ compound described by the XRD patterns. However, it is of interest to note the influence of nickel sulfate on the crystallization of $ZrTiO_4$ from the amorphous to the orthorhombic phase. As figure 3 shows, the exothermic peak due to the crystallization appears at 696 °C for $TiO_2$-$ZrO_2$, while for $NiSO_4/TiO_2$-$ZrO_2$ samples it is shifted to higher temperatures. The shift increases with increasing nickel sulfate content up to 20 wt%. Consequently, the exothermic peaks appear at 702 °C for 5-$NiSO_4/TiO_2$-$ZrO_2$, 708 °C for 10-$NiSO_4/TiO_2$-$ZrO_2$, 713 °C for 15-$NiSO_4/TiO_2$-$ZrO_2$, and 715 °C for 20-$NiSO_4/TiO_2$-$ZrO_2$. It was shown that the addition of sulfate, as well as titania as a second oxide to zirconia, hinders the crystallization of the originally amorphous preparation [28]. However, for the samples above 20 wt% of $NiSO_4$, the shift of the transition temperature did not continue to change. For the samples above 20 wt%, no further shift of the transition temperature suggests that the content of $NiSO_4$ exceeding 20 wt% does not interact with the surface of $TiO_2$-$ZrO_2$. For $NiSO_4/TiO_2$-$ZrO_2$, the endothermic peak around 790 °C is due to the evolution of $SO_3$ decomposed from the sulfate ion bonded to the surface of $TiO_2$-$ZrO_2$ [26]. However, for the 30- $NiSO_4/TiO_2$-$ZrO_2$ sample, two endothermic peaks are observed around 773 and 788 °C due to the evolution of $SO_3$, showing that sulfated species with different thermal stability are present in the samples [28].

### 3.4. Acidic properties of catalysts

The specific surface areas and number of acid sites of samples calcined at 500 °C for 1.5 h are listed in table 1. It is known that the catalytic activity of sulfated zirconia is rapidly lost due to sintering and coking. More active and stable catalysts can be obtained by addition of transition metal, especially noble metals [29–31]. The thermal resistance of zirconia against sintering can be considerably improved by incorporation a second oxide [32,33]. As listed in table 1, the surface area and number of acid sites of $TiO_2$-$ZrO_2$ binary oxide increased remarkably compared with pure titania and zirconia. It has been reported that the high surface acidity of the $TiO_2$-$ZrO_2$ binary oxide is attributed to the charge imbalance based on the generation of Ti—O—Zr bonding [18]. Yu et al. [34] has shown that $TiO_2$-$ZrO_2$ binary metal oxide exhibits higher catalytic activity than pure $TiO_2$, possibly due to an increase in surface area at a given calcination temperature and an increase in strength and/or number of acid sites. The surface area attained a maximum for 5-$NiSO_4/TiO_2$-$ZrO_2$, while the number of acid sites attained a maximum for 20-$NiSO_4/TiO_2$-$ZrO_2$.

Table 1
Specific surface area and number of acid sites of $NiSO_4/TiO_2$-$ZrO_2$ catalysts calcined at 500 °C

| Catalyst | Surface area ($m^2$/g) | Number of acid sites ($\mu$mol/g) |
|---|---|---|
| $TiO_2$ | 52 | 80 |
| $ZrO_2$ | 64 | 71 |
| $TiO_2$-$ZrO_2$ | 201 | 168 |
| 5-$NiSO_4/TiO_2$-$ZrO_2$ | 290 | 243 |
| 10-$NiSO_4/TiO_2$-$ZrO_2$ | 258 | 279 |
| 15-$NiSO_4/TiO_2$-$ZrO_2$ | 251 | 347 |
| 20-$NiSO_4/TiO_2$-$ZrO_2$ | 249 | 356 |
| 30-$NiSO_4/TiO_2$-$ZrO_2$ | 183 | 329 |
| 40-$NiSO_4/TiO_2$-$ZrO_2$ | 132 | 268 |

Figure 4 shows the infrared spectra of ammonia adsorbed on 20-$NiSO_4/TiO_2$-$ZrO_2$ samples evacuated at 500 °C for 1 h. The band at 1461 $cm^{-1}$ is the characteristic peak of an ammonium ion, which is formed on the Brönsted acid sites; the absorption peak at 1615 $cm^{-1}$ is contributed by ammonia coordinately bonded to Lewis acid sites [35,36], indicating the presence of both Brönsted and Lewis acid sites on the surface of the 20-$NiSO_4/TiO_2$-$ZrO_2$ sample. As figure 4(a) shows, the intense band at 1380 $cm^{-1}$ after evacuation at 500 °C is assigned to the asymmetric stretching vibration of

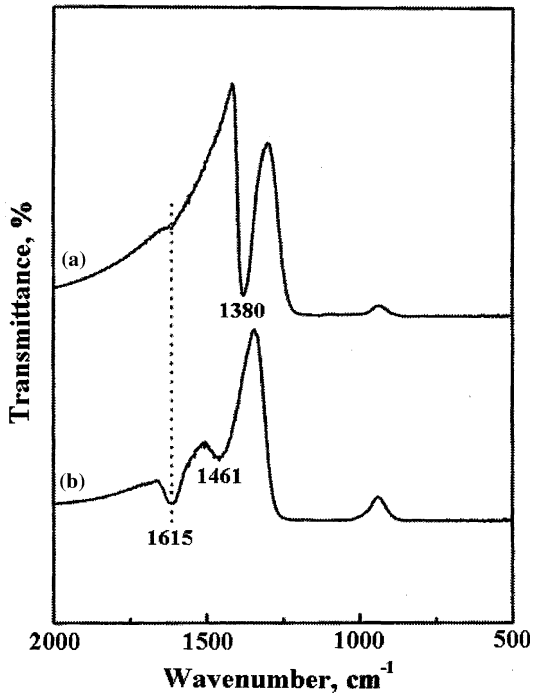


Figure 4. Infrared spectra of $NH_3$ adsorbed on 20-$NiSO_4/TiO_2$-$ZrO_2$: (a) background of 20-$NiSO_4/TiO_2$-$ZrO_2$ after evacuation at 500 °C for 1 h, (b) $NH_3$ adsorbed on (a), where gas was evacuated at 230 °C for 1 h.

S=O bonds having a high double bond character [23,24,28]. However, the drastic shift of the infrared band from 1380 $cm^{-1}$ to a lower wavenumber (not shown due to the overlaps of skeletal vibration bands of $TiO_2$-$ZrO_2$) after ammonia adsorption (figure 4(b)) indicates a strong interaction between an adsorbed ammonia molecule and the surface complex. Namely, the surface sulfur compound in the highly acidic catalysts has a strong tendency to reduce the bond order of S=O from a highly covalent double-bond character to a lesser double-bond character when a basic ammonia molecule is adsorbed on the catalysts [23,24]. Acids stronger than $Ho \leq -11.93$, which corresponds to the acid strength of 100% $H_2SO_4$, are considered 'superacids' [23,24]. The strong ability of the sulfur complex to accommodate electron from a basic molecule such as ammonia is indirectly related to the driving force to generate 'superacidic' properties [23,24]. Consequently, $NiSO_4/TiO_2$-$ZrO_2$ catalysts would be solid 'superacids', in analogy with the case of metal oxides modified with a sulfate groups [10,23,24]. This 'superacidic' property is attributable to the double bond nature of the S=O in the complex formed by the interaction between $NiSO_4$ and $TiO_2$-$ZrO_2$ [9,23,24].

### 3.5. Ethylene dimerization over $NiSO_4/TiO_2$-$ZrO_2$

$NiSO_4/TiO_2$-$ZrO_2$ catalysts were tested for their effectiveness in ethylene dimerization. It was found that for 20-$NiSO_4/TiO_2$-$ZrO_2$ and 40-$NiSO_4/TiO_2$-$ZrO_2$, ethylene was continuously consumed. This was shown by the results presented in figure 5, for catalysts that were evacuated at 500 °C for 1.5 h. Over $NiSO_4/TiO_2$-$ZrO_2$, ethylene was selectively dimerized to *n*-butenes. However, a small amount of hexenes from the phase adsorbed on the catalyst surface was detected. Therefore, the deactivation of catalyst occurred slowly due to the adsorption of oligomers. In the composition of *n*-butenes analyzed by gas chromatography, 1-butene was found to predominate exclusively at the initial reaction time, as compared with *cis*-butene and *trans*-butene. However, the amount of 1-butene decreases with the reaction time, while the amount of 2-butene increases. Therefore, it seems likely that the initially produced 1-butene is also isomerized to 2-butene during the reaction [4,9], $NiSO_4/TiO_2$-$ZrO_2$ was very effective for ethylene dimerization, but $TiO_2$-$ZrO_2$ without $NiSO_4$ exhibited absolutely no catalytic activity.

The catalytic activities of 20-$NiSO_4/TiO_2$-$ZrO_2$ were tested as a function of calcination temperature. The activities increased with the calcination temperature, reaching a maximum at 500 °C, after which the activities decreased. The decrease of catalytic activity after calcination above 500 °C seems to be due to the decomposition of sulfate ion bonded to $TiO_2$-$ZrO_2$, and/or the decrease of the surface area due to the formation of crystalline $ZrTiO_4$ at high calcination temperatures. In fact, the surface area of 20- $NiSO_4/TiO_2$-$ZrO_2$ calcined at 500 °C was found to be 249 $m^2/g$, but that of the sample calcined at 600 °C decreased to 154 $m^2/g$.

### 3.6. Correlation between catalytic activity and number of acid sites

The catalytic activities of $NiSO_4/TiO_2$-$ZrO_2$ catalysts calcined at 500 °C and containing different $NiSO_4$ were examined. The results are shown in figure 6, where

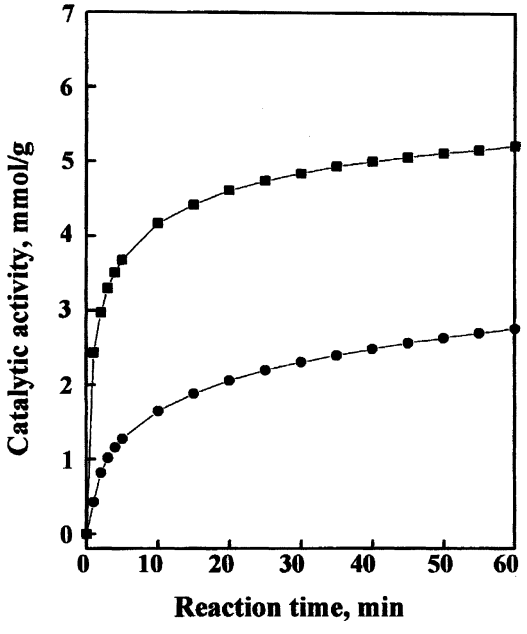


Figure 5. Time course of ethylene dimerization over catalysts evacuated at 500 °C for 1.5 h: ■ 20-$NiSO_4/TiO_2$-$ZrO_2$; ●, 40-$NiSO_4/TiO_2$-$ZrO_2$.

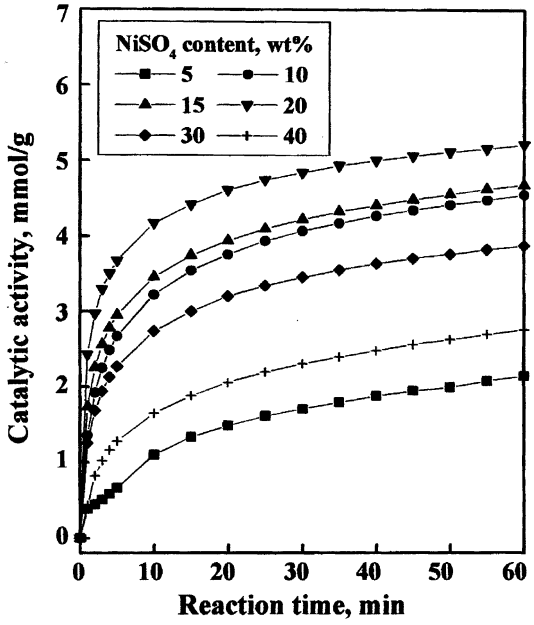


Figure 6. Catalytic activities of $NiSO_4/TiO_2$-$ZrO_2$ for ethylene dimerization as a function of $NiSO_4$ content.

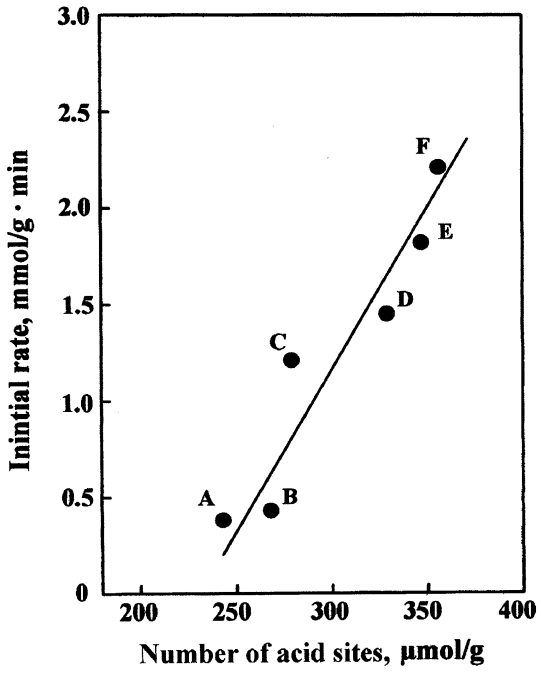


Figure 7. Correlationship between catalytic activity of $NiSO_4/TiO_2$-$ZrO_2$ for ethylene dimerization and number of acid sites. A, 5-$NiSO_4/TiO_2$-$ZrO_2$; B, 40-$NiSO_4/TiO_2$-$ZrO_2$; C, 10-$NiSO_4/TiO_2$-$ZrO_2$; D, 30-$NiSO_4/TiO_2$-$ZrO_2$; E, 15-$NiSO_4/TiO_2$-$ZrO_2$; F, 20-$NiSO_4/TiO_2$-$ZrO_2$.

catalysts were evacuated at 500 °C for 1.5 h before reaction. It was confirmed that the catalytic activity gives a maximum at 20 wt% of $NiSO_4$. This seems not to be correlated to the specific surface area, but closely correlated to the number of strong acid sites of catalysts.

The active sites responsible for ethylene dimerization consist of a low-valent nickel, $Ni^+$, and an acid site [9,37]. It has been also reported that the catalytic activity of nickel-containing catalysts in ethylene dimerization, as well as in butene isomerization, is closely correlated with the number of acid sites of the catalyst [4,8]. To examine the correlation between catalytic activity and acidity, the initial rates of $NiSO_4/TiO_2$-$ZrO_2$ containing different $NiSO_4$ contents are plotted as a function of the number of acid sites in figure 7, where catalysts were evacuated at 500 °C for 1.5 h before reaction. figure 7 shows a rough correlation between the catalytic activity and the number of acid sites. This rough correlation between the catalytic activity and the acidity can be explained by the dispersion of $NiSO_4$ on the surface and by the pore size of catalysts, where both influence the catalytic activity. In figure 7, the catalytic activity of 30-$NiSO_4/TiO_2$-$ZrO_2$ is lower than that of 20-$NiSO_4/TiO_2$ or 15-$NiSO_4/TiO_2$-$ZrO_2$. This is probably due to the lower dispersion of $NiSO_4$ caused by overloading of the $NiSO_4$ on the surface for the 30-$NiSO_4/TiO_2$-$ZrO_2$. Although the phase of $NiSO_4$ for 30- $NiSO_4/TiO_2$ -$ZrO_2$ is amorphous based on the result of the X-RD pattern, in view of the results for the surface and the number of acid sites of the sample in table 1, it is clear that the dispersion of $NiSO_4$ in 30-$NiSO_4/TiO_2$-$ZrO_2$ sample is not higher than that in 20-$NiSO_4/TiO_2$-$ZrO_2$ sample.

To examine the effect of pore size on the catalytic activity, the pore size of the catalysts calcined at 500 °C were measured. The average pore size of the catalysts decreased with increasing $NiSO_4$ loading. The mean pore diameter are 29, 24, 21, and 18 Å for the catalysts containing 5, 15, 20, and 30% $NiSO_4$, respectively. That is, pore size is narrowing as $NiSO_4$ loading increases. Therefore, it seems likely that the variation of pore size vs. $NiSO_4$ loading has an effect on the reaction rate of ethylene dimerization.

It is clear that the catalytic activity is a maximum at 20 wt% of $NiSO_4$. This seems to be correlated not to the specific surface area but to the number of acid sites of the catalysts. The acidty of $NiSO_4/TiO_2$-$ZrO_2$ calcined at 500 °C was determined by the amount of $NH_3$ irreversibly adsorbed at 230 °C [4,5]. As listed in table 1, the BET surface area attained a maximum extent when the $NiSO_4$ content in the catalyst was 5 wt% and then showed a gradual decrease with increasing $NiSO_4$ content. However, as shown in figure 7, the higher the number of acid sites, the higher the catalytic activity. In this way it is clear that the catalytic activity of $NiSO_4/TiO_2$-$ZrO_2$ is related to the acidity.

### 3.7. *Correlation between catalytic activity and asymmetric S=O stretching frequency*

The catalytic of 20-$NiSO_4/TiO_2$-$ZrO_2$ after evacuation at various temperatures were examined and the results are listed in table 2. The catalytic activity increased with an increase in evacuation temperature, reaching a maximum at 500 °C. To examine the effect of evacuation temperature on surface area, the BET surface area of 20-$NiSO_4/TiO_2$-$ZrO_2$ at various evacuation temperatures (300–600 °C) was measured. However, no change of surface area was observed, giving about 245–250 $m^2/g$ regardless of evacuation temperature. Therefore, it seems likely that the variation in catalytic activity relates not to the change in surface area but to the formation of active sites which depends on the evacuation temperature.

Table 2
Asymmetric stretching frequency of the S=O bonds, number of acid sites, and catalytic activity for 20-$NiSO_4/TiO_2$-$ZrO_2$ catalysts evacuated at different temperatures

| Evacuation temperatures (°C) | Frequency ($cm^{-1}$) | Number of acid sites ($\mu$mol/g) | Initial rate (mmol/g·min) | Turnover number (mmol/$\mu$mol·min×$10^3$) |
|---|---|---|---|---|
| 100 | 1350 | 48 | 0.20 | 4.2 |
| 200 | 1365 | 271 | 0.82 | 3.0 |
| 300 | 1374 | 320 | 1.16 | 3.6 |
| 400 | 1377 | 335 | 1.72 | 5.1 |
| 500 | 1380 | 356 | 2.21 | 6.2 |
| 600 | 1380 | 308 | 1.10 | 3.5 |

Comparing figure 1 and table 2, the catalytic activity closely correlates to the asymmetric stretching frequency of the S=O bonds. That is, the higher the infrared frequency of the S=O bonds, the higher the catalytic activity for ethylene dimerization. The decrease in catalytic activity after evacuation at 600 °C can be explained by the high evacuation temperature, resulting in the decrease in the number of sulfate groups bonded to the surface of $TiO_2$-$ZrO_2$. This is accompanied by the decrease in number of acid sites, as well as by the change the oxidation state of the nickel ion. An asymmetric frequency in the S=O bonds is a measure of the acid strength of a sulfur complexes ability to bond to basic molecules such as $H_2O$ and $NH_3$, and is related to the driving force which generates highly acidic properties, acid strength and the number of strong acid sites [9,25,26]. Both the acid strength and the number of acid sites increase with an increase in the evacuation temperature up to 500 °C, because water adsorbed on the catalyst surface is desorbed at high temperature, resulting in the formation of new acid sites and an increase in the bond order of S=O. Espinoza et al. [38] also reported that oligomerization activity of ethylene increased with an increase in acid strength of the support. The turnover number per number of acid sites is also listed in table 2. This shows a clear increase in the turnover number up to 500 °C, and then a drastic decrease due to the desorption of sulfate group at 600 °C. The turnover number per acid site is independent of the number of acid sites. Therefore, the increase in the turnover number means that the acid strength of the catalyst increases as the evacuation temperature increases up to 500 °C.

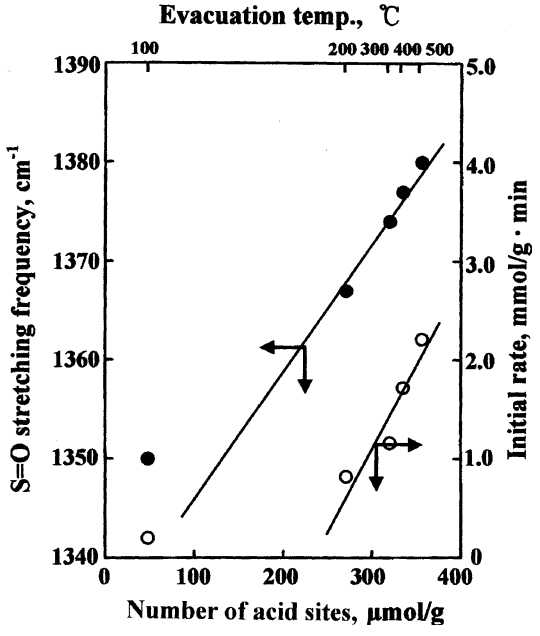


Figure 8. Correlationship among asymmetric stretching frequency of the S=O bonds, catalytic activity, and number of acid sites for 20-$NiSO_4$/$TiO_2$-$ZrO_2$, evacuated at different temperatures.

The frequency of the asymmetric S=O stretching vibration and catalytic activity of 20-$NiSO_4$/$IiO_2$-$ZrO_2$ after evacuation at different temperature were plotted against the acid amount in figure 8. There is good correlation among the infrared band frequency of the asymmetric S=O stretching vibration in $NiSO_4$/$TiO_2$-$ZrO_2$, catalytic activity for ethylene dimerization, the number of acid sites. Namely, the higher the frequency of the asymmetric S=O stretching vibration, the higher both the number of acid sites and the catalytic activity for ethylene dimerization. However, for sample evacuated at 100 °C, there is some deviation from the straight line above 200 °C, probably because the adsorbed water on the catalyst after evacuation at 100 °C influences both the catalytic activity and the number of acid sites. Therefore, it is concluded that we can use the asymmetric frequency of the S=O bonds in the $NiSO_4$/$TiO_2$-$ZrO_2$ catalyst as a measure of catalytic activity for ethylene dimerization.

## 4. Conclusions

The addition of nickel sulfate to $TiO_2$-$ZrO_2$ shifted the transition of $TiO_2$-$ZrO_2$ from an amorphous to an orthorhombic phase to a higher temperature because of the interaction between nickel sulfate and $TiO_2$-$ZrO_2$ surface. In addition, the number of acid sites of $NiSO_4$/$TiO_2$-$ZrO_2$ increased in proportion to the nickel sulfate content up to 20 wt% of $NiSO_4$. $NiSO_4$/$TiO_2$-$ZrO_2$ catalyst was very effective for ethylene dimerization as $TiO_2$-$ZrO_2$ without $NiSO_4$ does not exhibit any catalytic activity. 20-$NiSO_4$/$TiO_2$-$ZrO_2$ calcined at 500 °C exhibited the highest catalytic activity after evacuation at 500 °C. The high catalytic activity of $NiSO_4$/$TiO_2$-$ZrO_2$ was related to the increase of both the number of strong acid sites and the acid strength due to the addition of $NiSO_4$. The asymmetric stretching frequency of the S=O bonds for $NiSO_4$/$TiO_2$-$ZrO_2$ samples was related to the acidic properties and the catalytic activity; that is, the higher the frequency, the higher both the acidity and the catalytic activity.

## Acknowledgments

This work was supported by 2002 Research Fund of University of Ulsan and was partially supported by Grant No. (R05-2003-000-10074-0) from the Basic Research Program of the Korea Science Engineering Foundation. We wish to thank Korea Basic Science Institute (Daegu Branch) for the use of X-ray diffractometer.

## References

[1] K. Urabe, M. Koga and Y. Izumi, J. Chem. Soc. Chem. Commun. (1989) 807.

[2] F. Bernardi, A. Bottoni and I. Rossi, J. Am. Chem. Soc. 120 (1998) 7770.
[3] J.R. Sohn and A. Ozaki, J. Catal. 59 (1979) 303.
[4] J.R. Sohn and A. Ozaki, J. Catal. 61 (1980) 291.
[5] G. Wendt, E. Fritsch, R. Schöllner and H.Z. Siegel, Anorg. Allg. Chem. 467 (1980) 51.
[6] J.R. Sohn and D.C. Shin, J. Catal. 160 (1996) 314.
[7] G.F. Berndt, S.J. Thomson and G.J. Webb, J. Chem. Soc. Faraday Trans. 179 (1983) 195.
[8] T.V. Herwijnen, H.V. Doesburg and D.V. Jong, J. Catal. 28 (1973) 391.
[9] J.R. Sohn, W.C. Park and H.W. Kim, J. Catal. 209 (2002) 69.
[10] J.R. Sohn and W.C. Park, Bull. Kor. Chem. Soc. 21 (2000) 1063.
[11] G. Wendt, D. Hentschel, J. Finster and R. Schöllner, J. Chem. Soc. Faraday Trans. 179 (1983) 2013.
[12] K. Kimura and A. Ozaki, J. Catal. 3 (1964) 395.
[13] J.K. Maruya and A. Ozaki, Bull. Chem. Soc. Jpn. 46 (1973) 351.
[14] M. Hartmann, A. Pöppl and L. Kevan, J. Phys. Chem. 100 (1996) 9906.
[15] I.V. Elev, B.N. Shelimov and V.B. Kazansky, J. Catal. 89 (1984) 470.
[16] H. Choo and L. Kevan, J. Phys. Chem. B 105 (2001) 6353.
[17] K. Tannabe, T. Sumiyoshi, K. Shibata, T. Kiyoura and J. Kitagawa, Bull. Chem. Soc. Jpn. 47 (1974) 1064.
[18] J.C. Wu, C.S. Chung, C.L. Ay and I. Wang, J. Catal. 87 (1984) 98.
[19] J. Fung and F. Wang, J. Catal. 130 (1991) 577.
[20] E.P. Reddy, T.C. Rojas and A. Fernández, Langmuir 16 (2000) 4217.
[21] M.E. Zorn, D.T. Tompkins, W.A. Zeltner and M.A. Anderson, Appl Catal. B:Environ. 23 (1999) 1.
[22] J. Miciukiewicz, T. Mang and H. Knözinger, Appl. Catal. A 122 (1995) 151.
[23] T. Jin, T. Yamaguchi and K. Tanabe, J. Phys. Chem. 90 (1986) 4794.
[24] T. Yamaguchi, Appl. Catal. 61 (1990) 1.
[25] O. Saur, M. Bensitel, A.B.M. Saad, J.C. Lavalley, C.P. Tripp and B.A. Morrow, J. Catal. 99 (1986) 104.
[26] W. Hua, Y. Xia, Y. Yue and Z. Gao, J. Catal. 196 (2000) 104.
[27] R.V. Siriwardane, J.A. Poston Jr., E.P. Fisher, M.S. Shen and A.L. Miltz, Appl. Surf. Sci. 152 (1999) 219.
[28] J.R. Sohn and W.C. Park, Appl. Catal. A:Gen. 239 (2003) 269.
[29] K. Ebitani, J. Konishi and H. Hattori, J. Catal. 130 (1991) 257.
[30] V. Adeeva, G.D. Lei and W.M.H. Sachtler, Appl. Catal. 118 (1994) L11–L15.
[31] C.H. Lin and C.Y. Hsu, J. Chem. Soc. Chem. Commun 1479 (1992) .
[32] P.D.L. Mercera, J.G. van Ommen, E.B.M. Doesburg, A.J. Burggraaf and J.R.H. Ross, Appl. Catal. 57 (1990) 127.
[33] J.R. Sohn and S.G. Ryu, Langmuir 9 (1993) 126.
[34] J.C. Yu, J. Lin and R.W.M. Kwok, J. Phys. Chem. B 102 (1998) 5094.
[35] M.R. Basila and T.R. Kantner, J. Phys. Chem. 71 (1967) 467.
[36] A. Satsuma, A. Hattori, K. Mizutani, A. Furuta, A. Miyamoto, T. Hattori and Y. Murakami, J. Phys. Chem. 92 (1988) 6052.
[37] J.R. Sohn, W.C. Park and S.-E. Park, Catal. Lett. 81 (2002) 259.
[38] R.L. Espinoza, C.J. Korf, C.P. Nicolaides and R. Snel, Appl. Catal. 29 (1987) 195.